Numerical Modal Analysis of the Jet Wiping Instability

Miguel Alfonso Mendez[1] , Anne Gosset[2] , Kostas Myrillas[1], Jean-Marie Buchlin[1]

[1]von Karman Institute for Fluid Dynamics, EA Department, Rhode Sint-Genesius-Rode, Belgium

[2] Naval and Oceanic Engineering Deparment, A Coruña, Ferrol, Spain

Corresponding author: mendez@vki.ac.be

Key words: Air-Knife, Jet Wiping instability, LES-VOF for Two-Phase Flows, Modal Analysis

1. Introduction

This paper presents the second part of a study on the stability of the jet wiping process [1]. This process consists in using an impinging gas jet to control the coating thickness on a moving substrate, withdrawn from a coating bath. As shown in [2], this process is intrinsically unstable and characterized by a limited coating uniformity. While the interaction between the gas jet and the liquid is investigated experimentally in [1], this second part complements the previous works using computational fluid dynamics and modal analysis.

The jet wiping process is first reproduced on a 3D CFD simulation using the two-phase flow solver *interFoam* from the OpenFOAM package. The gas phase is solved with the Smagorinsky Large Eddy Simulation (LES) model, while the liquid phase is solved with the Volume of Fluid (VOF) method. The operating conditions corresponds to one of the experiments presented in the previous part, namely a strip velocity of $U_S = 0.34\, m/s$, a nozzle opening $d = 1.3mm$ a stand-off distance $Z = 10mm$ and a coating thickness $\hat{h}_f = h_f/\sqrt{v\, U_s/g} = 0.17$.

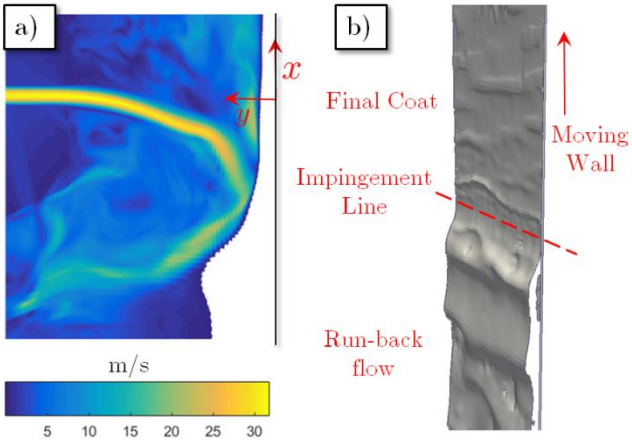

Figure 1: Examplary gas flow field sampled over a midplane of the 3D geometry and 3D reconstruction of the liquid interface showing the liquid film instability in the runback flow and in the final coat.

The computational domain is constructed by extruding the 2D geometry presented in [3] for a length of 30 mm. A detail of the gas jet impingement region from the simulation middle plane is shown in Fig.1a. As observed in the previous part of this work, the impinging jet flow develops sustained oscillations, periodically deflecting downward. On average, the jet flows appeared considerably tilted downward, with an average wiping location shift of about 2 mm. Fig.1b shows an instantaneous interface visualization, obtained as the isosurface with a volume fraction of 0.5. The formation of bidimensional waves in both the film flow downstream the impact (final) coat and upstream (run-back flow) is clearly visualized.

The dynamics of the liquid interface is analyzed by constructing the characteristic plane of the interface wave propagation, combining image processing and cross correlation analysis as described in Sec. 2. The dynamics of the impinging gas jet is investigated by means of Multiscale Proper Orthogonal (mPOD) decomposition [2-3], as described in Sec.3. Both investigations are carried out in the middle plane of the 3D simulations. The conclusions are presented in Sec.4.

2. Liquid Interface Analysis

From the sampled middle plane, the liquid film interface at each time step is retrieved via an image processing routine based on binarization and edge detection. These are carried out on the volume of fraction field, re-sampled on a uniform Cartesian grid and converted to an image. Three examples of interface reconstructions are shown in Fig. 2a together with the pressure field, revealing the impact position of the gas jet. These interface detection are used to construct the characteristic map $h(x,t)$ of the interface perturbation

in the time domain, shown in Fig.2.b, and in the frequency domain $\mathcal{H}(x,f) = \mathcal{F}\{h(x,t)\}$ with $\mathcal{F}$ the Fourier Transform, shown in Fig.2c. The spatio-temporal evolution in Fig. 2b displays two families of characteristic lines, originating from the wiping point ($x \approx -3mm$). The first propagates downstream, i.e. towards the final coat ($x \to +\infty$); the second propagates upstream, i.e towards the run back flow ($x \to -\infty$). A cross correlation analysis between the time signals at different positions reveals a propagation speed of $c_f = 0.24\ m/s$ towards the final coat and $c_r = -0.21\ m/s$ towards the run back flow. Interestingly a phase delay of $\Delta_t = -3.5ms$ is observed between the formation of the first with respect to the second. Concerning the wave frequency content, its spatial evolution in Fig.2c highlights two dominant frequencies, also visible by the merging and the bifurcation of several characteristic lines in Fig.2b. While both frequencies remain pronounced in the entire domain, the highest ($42\ Hz$) is more pronounced in the run-back flow while the lowest ($21\ Hz$) is better propagated in the final coat, in reasonable agreement with the light absorption measurements in [1, Fig. 5, for $\hat{h}_f = 0.2$].

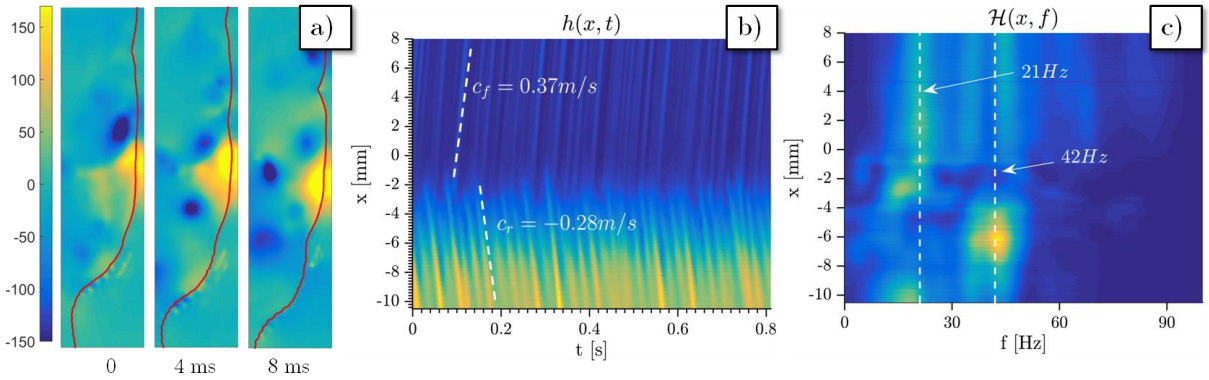

Figure 2: a) Examples of interface detection and corresponding pressure fields. b) Spatio-temporal evolution of the interface, displaying the characteristic lines propagating in the final coat and the run back flow. c) Spectra evolution as a function of the streamwise coordinate.

3. Gas Flow Modal Analysis via mPOD

The Multi-scale Proper Orthogonal decomposition proposed in [4] splits the dataset into a set of orthogonal modes, each having an energy σ_i^m, a spatial structure $\phi_i^m(x,y)$ and a temporal evolution $\psi_i^m(t)$ with limited frequency content, defined for a given scale m. Using Discrete Wavelet Transform (DWT), a multi-resolution analysis (MRA) is carried out on the time correlation tensor $K_{i,j} = \langle u(x,y,t_i), u(x,y,t_j) \rangle$, with $\langle .,. \rangle$ the correlation operator, to identify the contribution of each scale. Each of these contributions leads to a Proper Orthogonal Decomposition (POD) centered in the frequency bandwidth of the corresponding scale. The frequency spectrum of the correlation tensor, along with the band-pass region of two wavelet scales (m = 4,5) is shown in Fig.3a. The two dominant frequencies observed in the liquid flow are also visible in the spectra of the impinging gas jet. As the energy content in these two scales accounts for about 80% of the total energy, only the POD modes at these two scales are used to approximate the jet flow dynamics. This approximation removes broadband contribution due to turbulence and higher frequency phenomena.

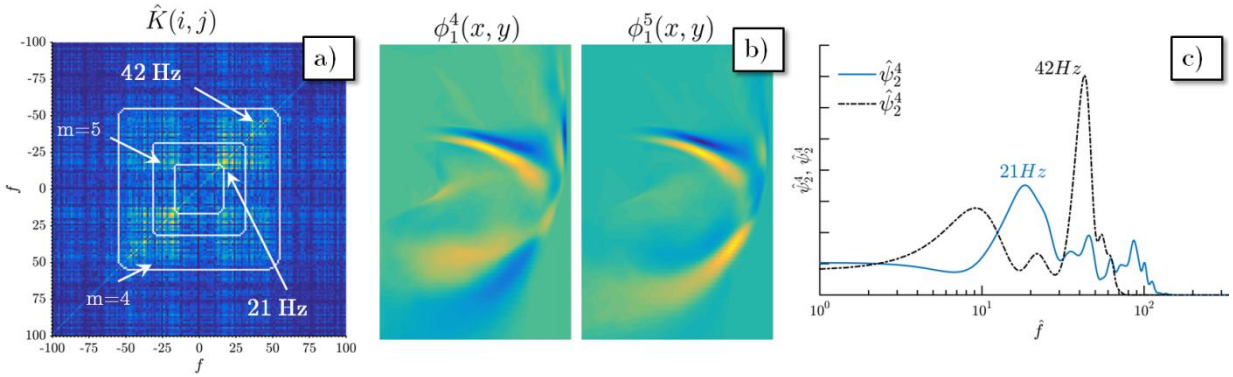

Figure 3: a) Fourier Transform of the correlation matric $K_{i,j}$, with the band-pass regions of two large wavelet scales. b) Dominant POD mode at the scale of the jet oscillation, displaying large recirculation underneath the jet flow. c) Spectrum of the dominant mode, pulsing at the frequency of the liquid film waves.

The spatial structures ϕ_1^4, ϕ_1^5 corresponding to the dominant POD modes at these two scales are shown in Fig. 3b; the frequency content of their corresponding temporal evolution $\hat{\psi}_1^4, \hat{\psi}_1^5$, with $\hat{\psi}_m^i = \mathcal{F}\{\psi_m^i(t)\}$, is shown in Fig. 3c. These two modes describe the dynamics of a large scale recirculation produced underneath the jet flow and responsible for the propagation of the run back flow pulsation to the impinging gas jet.

This approximation of the jet flow is used to reconstruct the large scale evolution of the pressure gradient distribution $\partial_x P(x,t)$ at the wall. The characteristic plane of such evolution is shown in Fig. 4a). The oscillation of the gas jet results in a pressure gradient which oscillates both in location x^* and maximum intensity $\partial_x P^*$. A tracking algorithm is developed to track this peak and the film thickness $h_f{}^*$ at its location. Fig. 4b shows an instantaneous profile of the dimensionless pressure gradient $\partial_x \hat{P} = \partial_x P/\rho g$ and the dimensionless thickness profile $\hat{h} = h/\sqrt{\mu U_S/(\rho g)}$ as function of the dimensionless stream-wise coordinate $\hat{x} = x/\sqrt{\mu U_S/(\rho g)}$.
The trajectory of the wiping point is shown in Fig.4c in the $\partial_x P^*(t)$-$h_f{}^*(t)$ plane and compared to the prediction of the 0D model of the jet wiping [5]. Although this model is derived under the assumption of lubrication theory and steady flow, its prediction remains reasonably close to the trajectory observed in dynamic conditions. It is therefore concluded that the pressure variations produced by the gas jet oscillation are sufficiently strong to produce undulation in the final coating film.

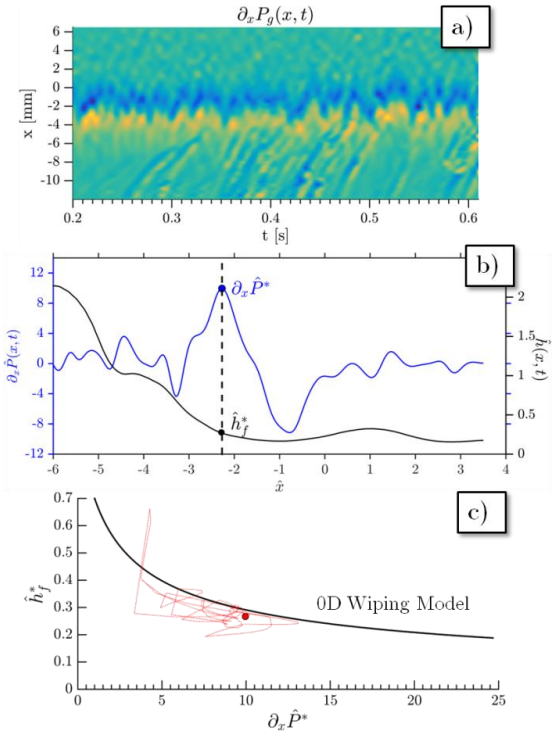

Figure 4: a) Evolution of the pressure gradient at the wall; b) instantaneous dimensionless film thickness and pressure gradient; c) orbit of the wiping point and comparison with the 0D wiping model.

4. Conclusions

A 3D LES-VOF simulation of the jet wiping process has been presented, and the results analyzed via multiscale Proper Orthogonal Decomposition (mPOD). The unstable wiping mechanism observed in [1,2] is revealed and the dynamics of the gas and the liquid flows are correlated. It is shown that the pulsations in the run-back liquid film can trigger and sustain an oscillation of the impinging jet, which is sufficiently strong to print undulation in the final coat.

Acknowledgements: We kindly acknowledge the Belgian F.R.S.-FNRS for the FRIA grant supporting M.A.Mendez and Arcelor-Mittal, for the financial support in this research project.

References

1. Gosset, A., Mendez, M.A., Buchlin, J.-M, *Experimental characterization of the jet wiping instability*, ECS 2017, Fribourg, Switzerland 2017.
2. Mendez, M.A., Gosset, A., Myrillas, K., Buchlin, J.-M, *A research methodology to study the jet wiping process*, ECS 2015, Eindhoven, the Netherland.
3. Myrillas, K., Rambaud, P., Mataigne, J.-M., Gardin, P., Vincent, S., Buchlin, J.-M., *Numerical modeling of gas-jet wiping process*, Chem. Eng. Process, Vol. 68, 2013, pp.26-31.
4. Mendez, M.A., Balabane, M., Buchlin, J.-M., *Multi-scale Proper Orthogonal Decomposition (mPOD)* ICNAAM, Thessaloniki, Greece 2017.
5. Gosset, A., Buchlin, J.-M., *Jet Wiping in Hot-Dip Galvanization*, J.Fluids Eng., 129(4), pp 466-475.